JBC RESEARCH ARTICLE

Citrus-derived DHCP inhibits mitochondrial complex II to enhance TRAIL sensitivity *via* ROS-induced DR5 upregulation

Received for publication, October 17, 2020, and in revised form, February 15, 2021 Published, Papers in Press, March 4, 2021,
https://doi.org/10.1016/j.jbc.2021.100515

Lei Chen, Miao Hao, Jingmin Yan, Lin Sun, Guihua Tai, Hairong Cheng*, and Yifa Zhou*

From the Engineering Research Center of Glycoconjugates Ministry of Education, Jilin Province Key Laboratory on Chemistry and Biology of Changbai Mountain Natural Drugs, School of Life Sciences, Northeast Normal University, Changchun, China

Edited by Dennis Voelker

Heat-modified citrus pectin, a water-soluble indigestible polysaccharide fiber derived from citrus fruits and modified by temperature treatment, has been reported to exhibit anticancer effects. However, the bioactive fractions and their mechanisms remain unclear. In this current study, we isolated an active compound, trans-4,5-dihydroxy-2-cyclopentene-l-one (DHCP), from heat-treated citrus pectin, and found that is induces cell death in colon cancer cells *via* induction of mitochondrial ROS. On the molecular level, DHCP triggers ROS production by inhibiting the activity of succinate ubiquinone reductase (SQR) in mitochondrial complex II. Furthermore, cytotoxicity, apoptotic activity, and activation of caspase cascades were determined in HCT116 and HT-29 cell-based systems, the results indicated that DHCP enhances the sensitivity of cancer cells to tumor necrosis factor–related apoptosis-inducing ligand (TRAIL), with DHCP-induced ROS accounting for the synergistic effect between DHCP and TRAIL. Furthermore, the combination of DHCP and TRAIL inhibits the growth of HCT116 and HT-29 xenografts synergistically. ROS significantly increases the expression of TRAIL death receptor 5 (DR5) *via* the p53 and C/EBP homologous protein pathways. Collectively, our findings indicate that DHCP has a favorable toxicity profile and is a new TRAIL sensitizer that shows promise in the development of pectin-based pharmaceuticals, nutraceuticals, and dietary agents aimed at combating human colon cancer.

Pectins are a family of galacturonic-acid-rich polysaccharides that include homogalacturonan, rhamnogalacturonan I and II, as well as xylogalacturonan. Pectins are complex polysaccharides abundant in the primary plant cell wall and are well known as dietary fibers. Previous studies have shown that various forms of pectin exhibit antitumor properties (1). Recently pH- and heat-modified pectins (MPs) demonstrated enhanced functions and bioactivities compared with native pectin. Notably, high-temperature-modified citrus pectin (HTCP) has been shown to induce apoptosis in androgen-responsive (LNCaP) and androgen-independent (LNCaP C4-2) human prostate cancer cells (2). HTCP also induces apoptosis-like cell death and autophagy in HepG2 and A549 cancer cells (3) and inhibits proliferation of human cancer cell lines, as well as the growth of sarcoma-180 tumors *in vitro* and *in vivo* (4). Our previous results showed that HTCP inhibits proliferation of some cancer cell lines, including HCT-116, HT-29, MDA-MB-231, S-180, HeLa, SMMC-7721, MCF-7, and HepG-2 cells (4). We also found that high-temperature-modified ginseng pectin induces apoptosis of HT-29 colon cancer cells *in vitro* (5), with similar results being observed with *Helianthus annuus* L. pectin *in vitro* and *in vivo* (6). It has also been reported that 4,5-dihydroxy-2-cyclopenten-1-one (DHCP), a bioactive compound isolated from HTCP, has a significant anticancer effect (7). However, the mechanisms for the anticancer effect of heat-modified pectin are still unclear.

Tumor necrosis factor (TNF)-related apoptosis-inducing ligand (Apo 2 or TRAIL/Apo2L) is a member of the TNF family of ligands capable of initiating apoptosis through engagement of its death receptors. TRAIL selectively induces apoptosis in a variety of tumor cells and transformed cells, but not in most normal cells, and therefore it has garnered intense interest as a promising agent for cancer therapy (8, 9). However, the primary and acquired resistance of cancer cells to TRAIL has become a roadblock of TRAIL therapy. Hence, the combination of other therapies with TRAIL to overcome this resistance has become a promising strategy. TRAIL exerts remarkable antitumor activity in combination with cytotoxic drugs in phase I and phase II clinical trials (9, 10). It is noteworthy that several natural pharmacological agents have shown the potential to sensitize cancer cells to TRAIL-induced apoptotic activity *via* reactive oxygen species (ROS) production and thus has made the main appealing therapeutic option in combination with recombinant TRAIL or DRs-agonist antibodies (10–14).

In current study, we isolated DHCP from HTCP and investigated its effect on colon cancer inhibition and its mechanism of action. The synergistic effect of DHCP and TRAIL, as well as possible mechanisms underlying their synergistic effect, was also investigated. These findings offer evidence for DHCP as a new TRAIL sensitizer and promise for the development of pectin-based pharmaceuticals,

* For correspondence: Hairong Cheng, chenghr893@nenu.edu.cn; Yifa Zhou, zhouyf383@nenu.edu.cn.

nutraceuticals, and dietary additive in the combat against human colon cancer.

Results

Preparation and detection of DHCP

HTCP, along with its fractions HTCP-S, HTCP-P, HTCP-S-IS, HTCP-S-OS, HTCP-S-OS1, HTCP-S-OS2, and HTCP-S-OS3, was obtained according to the method described (Fig. 1*A*). Human colon cancer HCT-116 cells were treated with these fractions for 24 h, and cell viability was assessed using the WST-1 assay. Data showed that cell viability was slightly impaired by CP, HTCP-P, HTCP-S-IS, HTCP-S-OS1, and HTCP-S-OS2, but significantly inhibited by HTCP, HTCP-S, HTCP-S-OS, and HTCP-S-OS3 (Fig. 1, *B–D* and Fig. S1). HTCP-S-OS3 exhibited the most significant cell viability inhibitory activity among all fractions from HTCP. These results indicate that active compounds are present in the HTCP-S-OS3 fraction. Hence, HTCP-S-OS3 was further separated by HPLC (Kromasil C18 column) into fractions F1, F2, and F3 (Fig. 1*A*). Our results show that whereas F1 and F2 exhibited cell viability inhibitory effects with IC50 values of 16 and 26 μg/ml, respectively, fraction F3 had an IC50 value of 4 μg/ml, much lower than F1 or F2 (Fig. 1*E*). This suggested that F3 is the primary contributor to the activity of the HTCP-S-OS3 fraction. Structure elucidation of relatively pure fraction

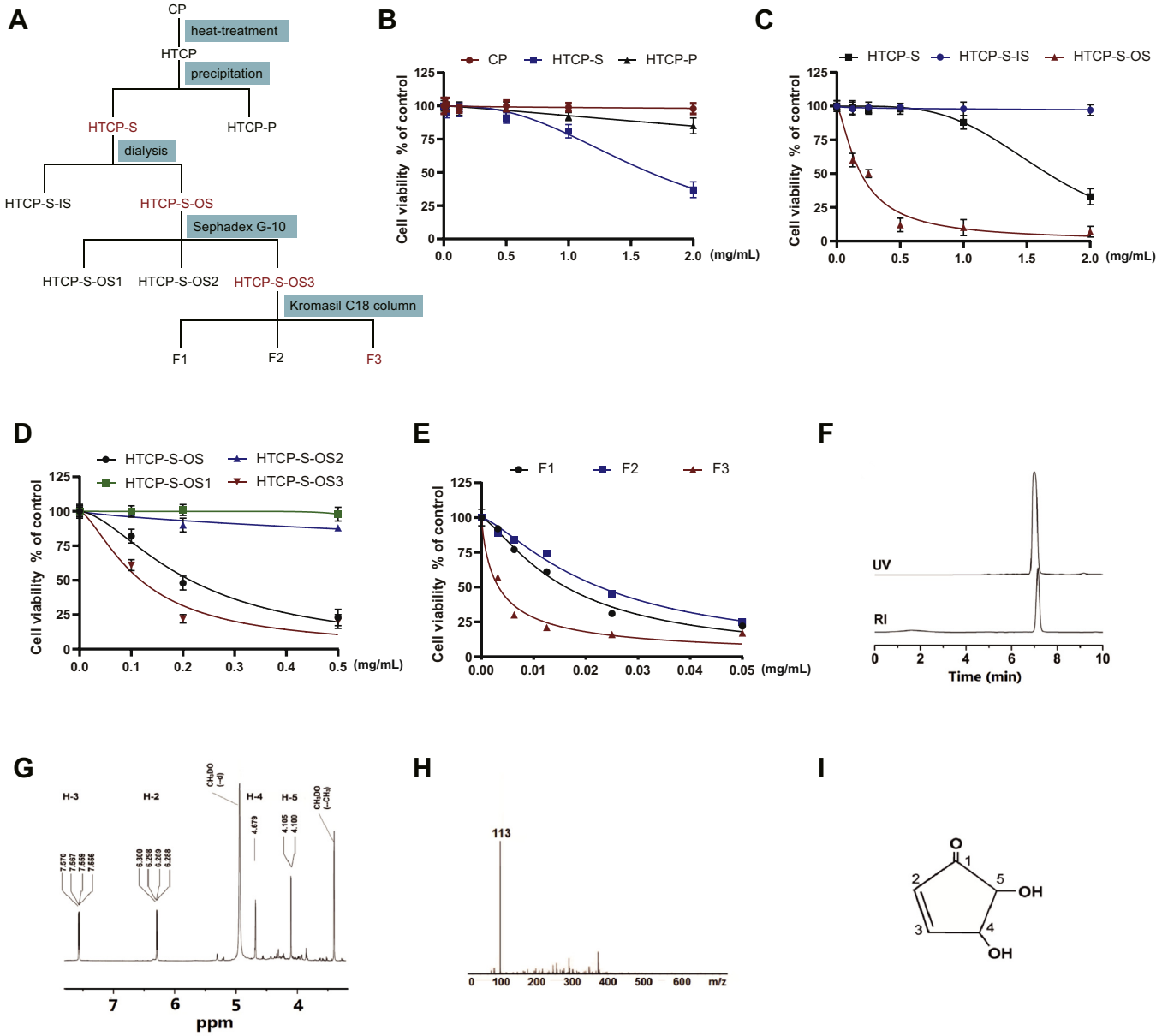

Figure 1. Preparation and detection of DHCP. *A*, preparation and detection of DHCP. *B–E*, the anticancer effects of CP and fractions of HTCP on HCT-116 human colon cancer cells. Cells were treated with different concentrations of CP, HTCP-S, and HTCP-P (*B*) or HTCP-S, HTCP-S-IS, and HTCP-S-OS (*C*) or HTCP-S-OS, HTCP-S-OS1, HTCP-S-OS2, and HTCP-S-OS3 (*D*) or F1, F2, and F3 (*E*) for 24 h. Cell proliferation was assessed for each condition by MTT assay. *F–I*, structural characterization of F3. *F*, elution profiles of F3 on a HPLC Kromasil C18 column. *G*, ^{1}H NMR spectrum of F3. *H*, mass spectrum of F3. *I*, molecular structure of DHCP. RI, refractive index detector; UV, ultraviolet detector.

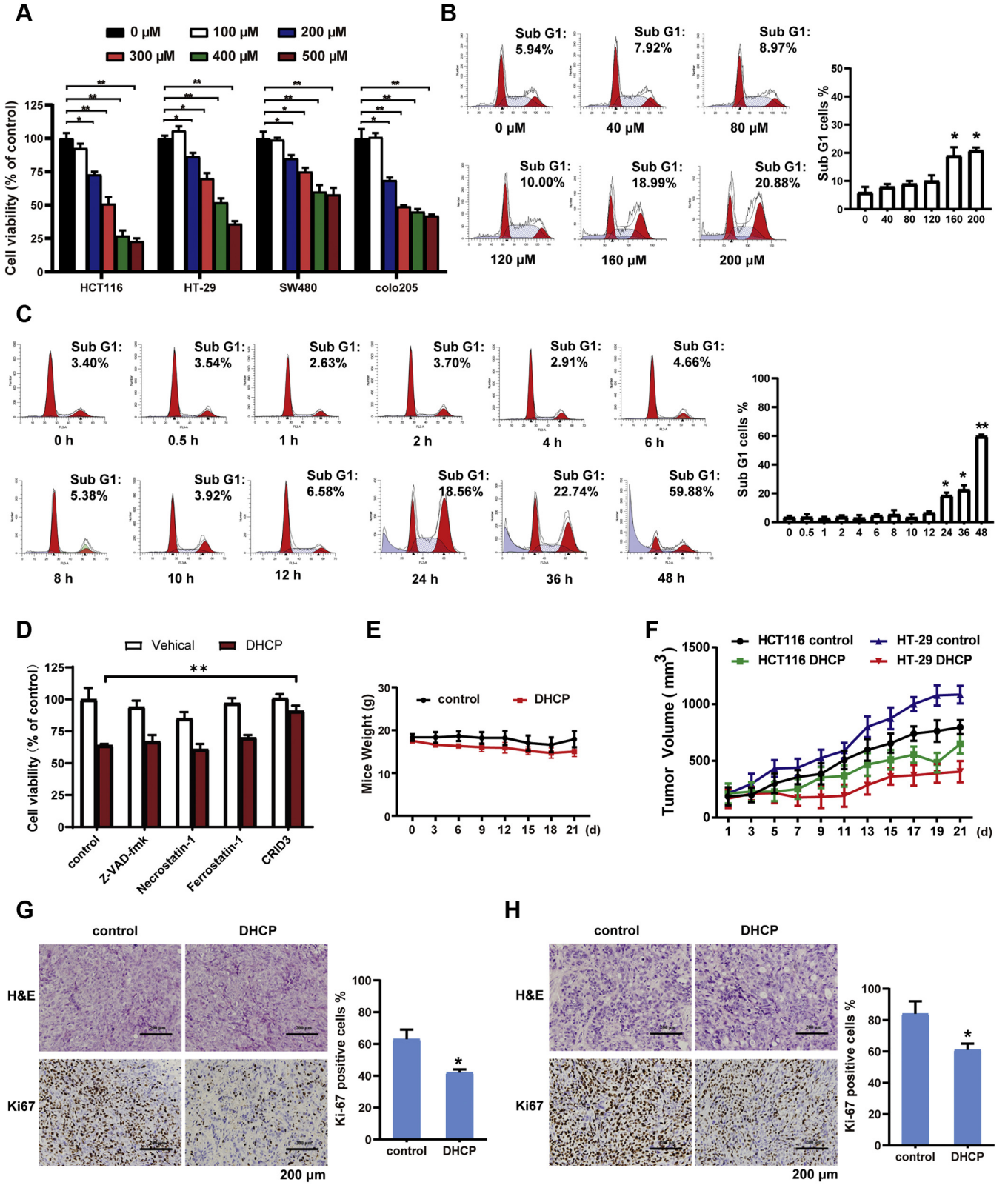

Figure 2. DHCP inhibits human colon cancer *in vitro* and *in vivo*. *A*, four colon cancer cell lines were treated with indicated concentrations of DHCP for 24 h. Cell viability was assessed using WST-1 assay. Quantitative analysis of cell viability (means ± SD, n = 3) from three experiments. *B* and *C*, HCT116 cells were treated with indicated concentrations of DHCP for 24 h (*B*) or treated with 200 μM of DHCP for indicated times, (*C*) and cell death was tested by flow cytometry. *D*, HCT116 cells were pretreated with Z-VAD-FMK (20 μM), Necrostatin-1 (10 μM), Ferrostatin-1 (1 μM), and CRID3 (1 mM) for 1 h, followed by 24 h of DHCP treatment. Cell viability was assessed using WST-1 assay. *E–H*, nude mice bearing HCT116 and HT-29 xenograft tumors were treated with 0.5 mg/kg of DHCP every other day. Animals were treated with ten consecutive cycles. Mice weight (*E*) and tumor volume (*F*) were then measured. The expressions of Ki-67 of HCT116 (*G*) and HT-29 (*H*) tumor tissues were tested by immunohistochemistry staining. Statistical significance was determined with Student's *t*-test (*$p < 0.05$, **$p < 0.01$).

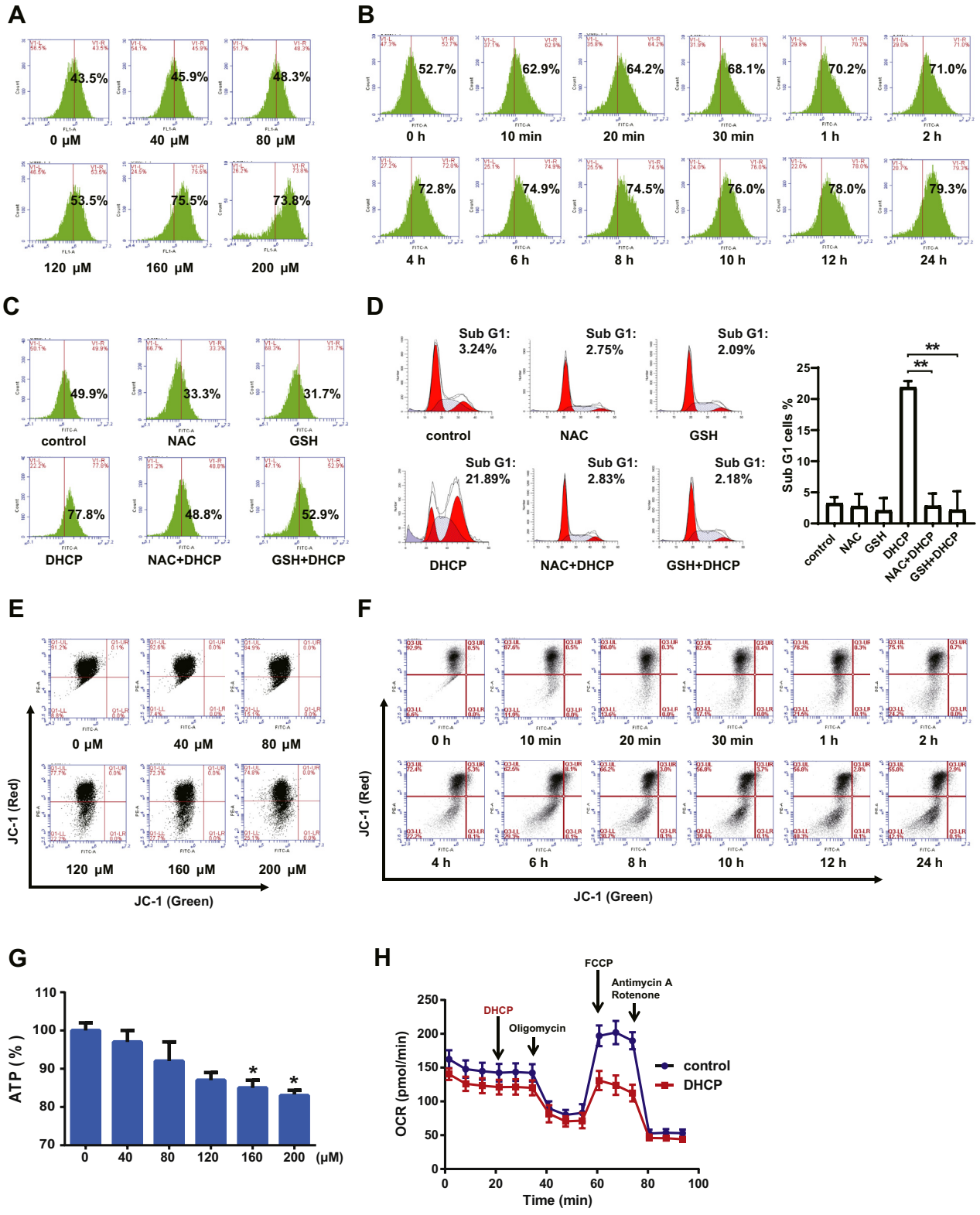

Figure 3. Generation of mitochondrial ROS induced by DHCP was responsible for the cell death of colon cancer cells. *A* and *B*, HCT116 cells were treated with indicated concentrations of DHCP for 24 h (*A*) or treated with 200 μM of DHCP for indicated times (*B*). ROS levels were assessed by flow cytometry after stained by DCFH-DA. *C* and *D*, HCT116 cells were pretreated with NAC or GSH for 1 h and then treated with 200 μM of DHCP for 24 h, the ROS levels (*C*) and cell death (*D*) were assayed by flow cytometry. *E* and *F*, HCT116 cells were treated with indicated concentrations of DHCP for 24 h (*E*) or treated with 200 μM of DHCP for indicated times (*F*). Mitochondrial membrane potential was analyzed by flow cytometry after stained by JC-1. *G*, HCT116 cells were treated with indicated concentrations of DHCP for 1 h, the ATP production was analyzed using the ATP assay kit. *H*, HCT116 cells were treated with 200 μM of DHCP for 1 h, the mitochondrial aerobic respiration was measured. Statistical significance was determined with Student's *t*-test (*$p < 0.05$).

F3 (Fig. 1*F*) showed that its chemical structure analyzed by ^{1}H NMR (Fig. 1*G*) has four dominant resonances at 7.56 ppm [1 H, dd, *J* = 1.8 Hz, 2-H], 6.28 ppm [1 H, dd, *J*= 1.2 Hz, 3-H], 4.68 ppm [1 H, m, 4-H], and 4.10 ppm [1 H, d, *J* = 3.0 Hz, 5-H]. The mass spectrum (MS) of F3 shows the primary fragment ion at 113 [M-H] (Fig. 1*H*). These results suggest that F3 is DHCP (Fig. 1*I*).

DHCP inhibits the growth of human colon cancer cells in vitro *and in mouse xenografts*

The cytotoxicity of DHCP on human colon cancer cells has never been reported. Here, we found that DHCP demonstrates a dose-dependent inhibitory effect on four colon cancer cell lines (Fig. 2*A*) and induces cell death of HCT116 cells in a dose- and time-dependent manner (Fig. 2, *B* and *C*). We found that DHCP initiates the processing of caspase-3, -8, -9, and PARP in HCT116 also in dose- and time-dependent manners (Fig. S2, *A* and *B*). However, cell death induced by DHCP could not be inhibited by Z-VAD-FMK. To investigate pathways involved in DHCP-mediated cell death in greater detail, we investigated various types of cell death inhibitors. Our results show that cell death was also not impacted by pretreatment with necrosis inhibitor necrostatin-1 or ferroptosis inhibitor ferrostatin-1 (Fig. 2*D*). In contrast, the inflammasome inhibitor CRID3 could restore cell viability (Fig. 2*D*). Collectively, these data suggest that DHCP-induced cell death is mediated by a pathway dependent on pyroptosis. Moreover, DHCP suppressed the growth of HCT116 and HT-29 xenografts without impacting body weight, suggesting the lack of cytotoxicity (Fig. 2, *E*–*H*).

Generation of mitochondrial ROS induced by DHCP is responsible for the death of colon cancer cells

Moderate increases of ROS contribute to tumor promotion and progression. However, ROS can also trigger programmed cell death. Cancer cells exhibit higher ROS levels than normal cells; consequently, cancer cells are more vulnerable to oxidative stress than are normal cells. This can be utilized as an anticancer strategy. In the present study, we found that DHCP induces robust generation of ROS in HCT116 cells in a dose- and time-dependent manner (Fig. 3, *A* and *B*). ROS scavengers (NAC or GSH) significantly decrease ROS induced by DHCP (Fig. 3*C*), as well as cell death induced by DHCP (Fig. 3*D*). Mitochondria are regarded as the primary source for ROS (15) that can be triggered by deficient antioxidants, inhibition of electron flow, or exposure to xenobiotics. Several xenobiotics have been reported to increase the rate of ROS production by interacting with the mitochondrial electron pathway (16). To investigate whether ROS production induced by DHCP is generated through the mitochondrial pathway, the mitochondrial transmembrane potential (MMP) was assessed by flow cytometry followed by JC-1 staining. Our results show that DHCP lowers MMP in a concentration- and time-dependent manner (Fig. 3, *E* and *F*). Mitochondria are the principal site of important cellular functions, including ATP production *via* oxidative phosphorylation (17). DHCP also exhibited a significantly inhibitory effect on mitochondrial ATP production (Fig. 3*G*). In addition, the mitochondrial oxidative phosphorylation function upon DHCP treatment was determined by detecting the oxygen consumption rate. The results showed that DHCP exerted a robust inhibitory effect on oxidative phosphorylation of HCT116 (Fig. 3*H*), HT-29, SW480, DLD-1, and colo205 colon cancer cell lines (Fig. S3). These results suggest that DHCP induces ROS generation by influencing the mitochondrial activity. To confirm this, we examined the effects of DHCP on ROS levels in normal A549 cells and A549 ρ0 cells in which mitochondrial function was negated by depletion of mtDNA (18). Upon DHCP treatment, cellular ROS levels increased from 49.1% to 73.5% in A549 cells, whereas it remained basically unchanged in A549 ρ0 cells (Fig. S4), supporting the hypothesis that DHCP induces ROS generation by modulating mitochondrial activity.

Inhibition of mitochondrial complex II activity by DHCP contributes to ROS generation

The mitochondrial respiratory chain is the major cellular generator of superoxide and associated ROS as electrons leak from sites at or within respiratory chain complexes (19). Complexes I and III have long been recognized as the main sources of ROS. In recent years, complex II has also been established as an efficient producer of ROS (20). Here, HCT116 cells were permeabilized by digitonin (0.001%) and then were loaded with specific substrates to dissect the multiple steps of aerobic respiration and examined by using Seahorse XFp Extracellular Flux Analyzers as described in literature (21). Activity of mitochondrial complex I was measured by using glutamine as substrate, which ultimately produces NADH for complex I oxidation. The results showed that glutamine-driven aerobic respiration was unaffected on DHCP-treated cells (Fig. 4*A*), suggesting that DHCP could not inhibit complex I activity.

Next, the impact of DHCP on the activity of complex II was evaluated. The complex I activity was inhibited by rotenone, and then succinate was used as substrate to measure the cellular response to complex II activity. As shown in Figure 4, *A*–*C*, DHCP significantly inhibited the aerobic respiration dependent on succinate, suggesting that DHCP is the inhibitor of complex II.

The activity of complex III was measured with the substrate glycerol-3-phosphate (G-3-P) according to previous report (21). As shown in Figure 4*B*, DHCP had no effect on the oxygen consumption driven by G-3-P, suggesting no effect on complex III activity.

Tetramethyl-*p*-phenylene diamine (TMPD) was used as the substrate to determine the effect of DHCP on the activity of complex IV. TMPD can donate electrons directly to complex IV to reduce O_2. In the presence of indicated inhibitors (rotenone, malonate, and antimycin A) to complex I, complex II, and complex III, DHCP did not change the oxygen consumption caused by the oxidation of TMPD, indicating that complex IV was not affected by DHCP (Fig. 4*C*).

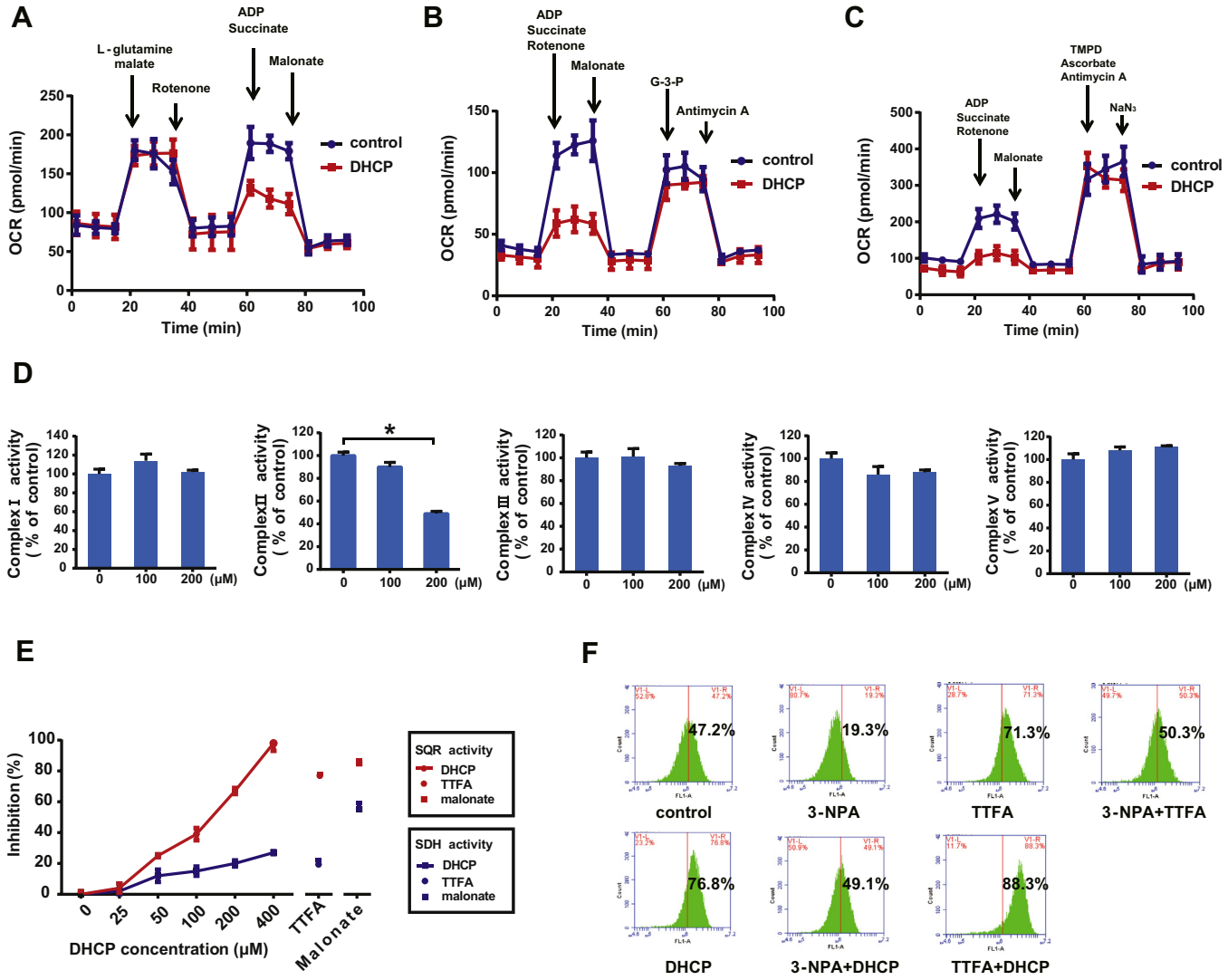

Figure 4. DHCP inhibits complex II by interfering with ubiquinone reduction to induce ROS generation. *A–C*, HCT116 cells were treated with 200 μM of DHCP for 1 h, then incubated with 0.001% digitonin dissolved in MAS buffer to selectively permeabilize plasma membrane. Different oxidizable substrates and inhibitors were added into the cells as indicated and the mitochondrial aerobic respiration was measured. For measurement of complex II activity, 10 mM L-glutamine + 10 mM malate was used as oxidizable substrate. For measurement of complex II activity, complex II was inhibited by rotenone; 10 mM succinate +4 mM ADP was used as oxidizable substrate. For measurement of complex III activity, complexes I and II were inhibited using rotenone and malonate, respectively; 5 mM glycerol-3-phosphate was used as oxidizable substrate. For measurement of complex IV activity, complexes I, II, and III were inhibited using rotenone, malonate, and antimycin A, respectively; 10 mM ascorbate +100 mM TMPD was used as oxidizable substrate. *D*, HCT116 cells were treated with 200 μM of DHCP for 1 h, then the mitochondria were isolated, and the activity of mitochondrial complexes was analyzed using the MitoCheck complex activity assay kits, respectively. *E*, isolated HCT116 mitochondria were incubated with indicated concentrations of DHCP, TTFA (150 μM), or malonate (10 mM). SQR and SDH activities were measured as described in the method. *F*, HCT116 cells were treated with DHCP (200 μM), 3-NPA (500 μM), or TTFA (150 μM) in different combinations, ROS levels were assessed by flow cytometry after stained by DCFH-DA. Statistical significance was determined with Student's *t*-test (*$p < 0.05$).

To further demonstrate that DHCP inhibited complex II activity, mitochondrial complex activities were also evaluated *in vitro*, in which the activity of complex II, but not of complexes I, III, IV, and V, was markedly reduced upon DHCP treatment (Fig. 4*D*).

Mechanism of complex II inhibition by DHCP

Mitochondrial complex II (succinate dehydrogenase; SDH) contains four subunits (SDHA, SDHB, SDHC, and SDHD). The enzyme activities of SDH include SDH (succinate dehydrogenase) and SQR (succinate ubiquinone reductase) activities (22). Electrons resulting from the oxidation of succinate within SDHA are transferred from SDHA-bound flavin adenine dinucleotide cofactor to Fe-S clusters of SDHB and finally to the ubiquinone reduction site residing between SDHC and SDHD where ubiquinone is reduced to ubiquinol (23). To determine the specificity of complex II inhibition by DHCP, the activities of SDH and SQR were measured as previously reported (23). Complex II inhibitors TTFA and malonate were used to determine the specificity of the SQR and SDH activity assays. TTFA inhibits complex II activity by primarily binding to the ubiquinone-binding site, whereas malonate competes with succinate for the dehydrogenase-binding site on complex II. Here we found that DHCP

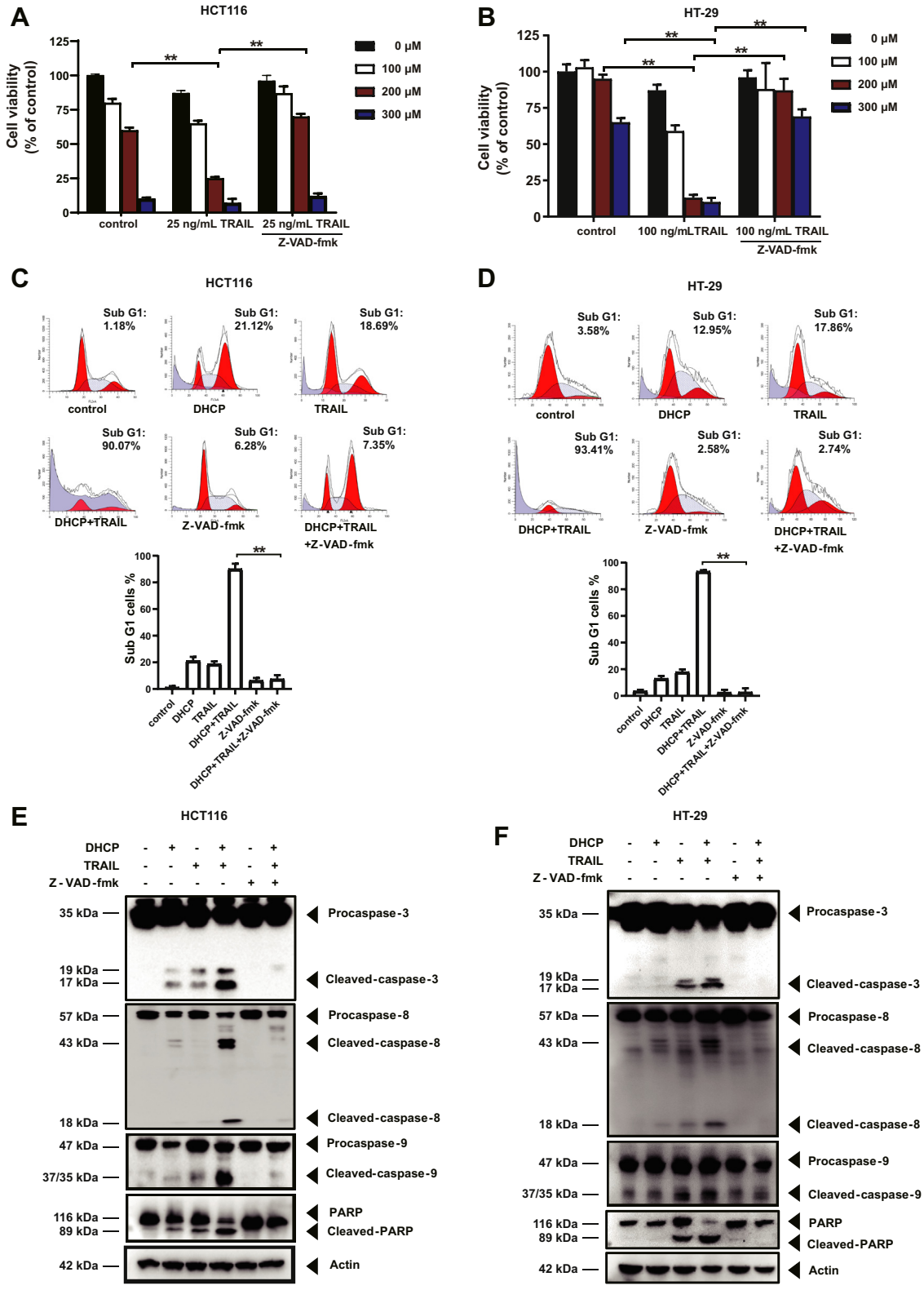

Figure 5. DHCP sensitizes colon cancer cells to TRAIL. *A* and *B*, HCT116 (*A*) and HT-29 (*B*) cells were pretreated with or without 20 μM Z-VAD-FMK for 1 h and then cotreated with or without indicated doses of DHCP and TRAIL for 24 h. Cell viability was analyzed with WST-1 assay. *C* and *D*, HCT116 (*C*) and HT-29 (*D*) cells were pretreated with or without 20 μM Z-VAD-FMK for 1 h and then cotreated with or without indicated doses of DHCP and TRAIL for 24 h. Cell death was tested by flow cytometry after stained by PI. (E and F) HCT116 (E) and HT-29 (F) cells were pretreated with or without 20 μM Z-VAD-FMK for 1 h and then cotreated with or without indicated doses of DHCP and TRAIL for 24 h. The processing of caspases and PARP were tested by western blot. Error bars in *A* and *B* represent the SD. (N = 3 independent experiments). $^{*}p < 0.05$, $^{**}p < 0.01$ compared with control group (Student's *t*-test, two-tailed).

suppressed both SQR and SDH activities in a dose-dependent manner. However, the inhibitory effect of DHCP on SQR activity was much more prominent than that of SDH (Fig. 4*E*). The effect of DHCP is identical to that of TTFA, but not of malonate (Fig. 4*E*), suggesting that DHCP inhibits complex II activity and may interfere with ubiquinone reduction, possibly at the ubiquinone-binding site in SDHC and SDHD. To confirm this, cellular ROS generation was examined after cotreatment with TTFA (or complex II inhibitor 3-NPA) and DHCP. It had been reported that 3-NPA abrogates ROS generation by binding to the active site of SDHA and inhibiting electron transfer from succinate to FAD. Consistent with previous reports, our results show that 3-NPA decreases ROS generation and reduces ROS production triggered by TTFA (Fig. 4*F*). In contrast, cotreatment of DHCP and TTFA exerts an additive effect on ROS production, whereas 3-NPA markedly decreases the level of ROS generation by DHCP (Fig. 4*F*). These results confirmed that DHCP inhibits complex II by interfering with ubiquinone reduction.

DHCP sensitizes colon cancer cells to TRAIL

Increased ROS levels are thought to impair drug resistance of cancer cells. Here, we found that DHCP sensitizes three clinical anticancer drugs (5-fluorouracil, irinotecan, oxaliplatin) and one preclinical drug TRAIL. DHCP slightly synergizes with 5-FU, irinotecan, or oxaliplatin, but shows a significant synergistic effect with TRAIL (Fig. S5). We further investigated the synergistic effect on TRAIL-sensitive HCT116 cells and TRAIL-resistant HT-29 cells. Our results show that HCT116 and HT-29 cells are modestly or minimally sensitive to either DHCP or TRAIL alone (Fig. 5, *A* and *B*). However, their combination significantly decreases the viability of HCT116 and HT-29 cells (Fig. 5, *A* and *B*). In contrast, DHCP enhances TRAIL-induced cell death in other colon cancer cells as well (Fig. S6). However, DHCP and TRAIL showed minimal synergistic effect on human colonic epithelial NCM460 cells (Fig. S7). These results suggest that combination of DHCP and TRAIL might preferentially target cancer cells. Our FACS results show that DHCP or TRAIL alone induces 21.1% and 18.7% cell death, respectively. The combination treatment promoted apoptosis to 90% (Fig. 5*C*). For HT-29 cells, DHCP and TRAIL treatment alone induced 13% and 18% cell death, respectively. The combination treatment enhanced cell death to 93.4% (Fig. 5*D*). Consistently, the combination of DHCP and TRAIL more efficiently initiated the processing of caspase-3, -8, -9, and PARP in HCT116 and HT-29 cells (Fig. 5, *E* and *F*). Moreover, cell death (Fig. 5, *C* and *D*) and cleavage of caspase-3, -8, -9, and PARP (Fig. 5, *E* and *F*) induced by DHCP and TRAIL were effectively blocked by pretreatment with Z-VAD-FMK, indicating that DHCP sensitizes human colon cancer cells to TRAIL-induced cell death in a caspase-dependent manner.

DHCP enhances TRAIL sensitivity in vivo

The therapeutic combination of DHCP and TRAIL was also tested *in vivo*. Mice bearing xenografted HCT116 and HT-29 colon tumor cells were treated with DHCP and/or TRAIL every other day. These results indicate that combination therapy did not impact the weight of the mice (Fig. S8*A*), but did significantly suppress tumor growth (Fig. 6, *A* and *B*), tumor size (Fig. S8*B*), and tumor volume (Fig. S8*C*). The expression of ki-67 and cleaved-caspase-3 in tumor tissue samples also demonstrated that DHCP and TRAIL exerted a synergistic effect (Fig. 6, *C* and *D*).

DHCP suppressed expression of cell survival proteins and induced expression of procell death proteins

To identify the mechanism by which DHCP sensitizes colon cancer cells to TRAIL, we investigated multiple extrinsic and intrinsic cell death pathway components that could be affected by DHCP. The results showed that DHCP decreased the expression of cell survival proteins, including Bcl-2, cFLIP, Mcl-1, c-IAP1, c-IAP2, XIAP, survivin, and Livin, whereas it increased procell death proteins including Bax, tBid, and Cyt-c (Fig. 7, *A* and *B*). These changes may account, at least in part, for the synergistic effect.

DHCP induces the expression of DR5

Decreased expression of TRAIL receptors DR4 and DR5 accounts for TRAIL resistance in certain cancer cell lines. DR5, but not DR4, was upregulated upon DHCP treatment in a dose-dependent manner (Fig. 7*C*). Consistent with protein changes, DHCP treatment increased DR5 cell surface expression (Fig. 7*D*). Moreover, upregulation of DR5 is indeed mediating the observed cooperative effect between DHCP and TRAIL. To substantiate this, two specific siRNAs of DR5 were applied to silence DR5 expression (Fig. 7, *E* and *F*). Upon DR5 siRNAs transfection, cell death induced by the combination of DHCP and TRAIL was decreased from 96.7% to 67.8% or 60.8%, respectively (Fig. 7*G*). Collectively, we conclude that DR5 upregulation by DHCP plays a crucial role in the synergistic effect of DHCP and TRAIL.

In this study, we were particularly interested in the mechanism of action accounting for the upregulation of DR5 in response to DHCP. The reason is that agonistic TRAIL-R antibodies that selectively target DR5 induce apoptosis by the same mechanism as TRAIL. However, the stability of TRAIL-R antibodies *in vivo* makes them attractive agents for use in humans, and several clinical trials investigating TRAIL-R antibodies in solid and hematological tumors have been initiated. The upregulation of DR5 provides a possibility for the combination of DHCP and TRAIL-R antibodies. We next sought to identify pathways involved in DHCP-induced DR5 upregulation.

DHCP increases DR5 expression in a p53-CHOP-dependent pathway

Our results, along with those of other researchers, have shown that p53 and CHOP are involved in DR5 upregulation (24). In the present study, we found that DHCP induces the upregulation of p53 and CHOP in a dose- and

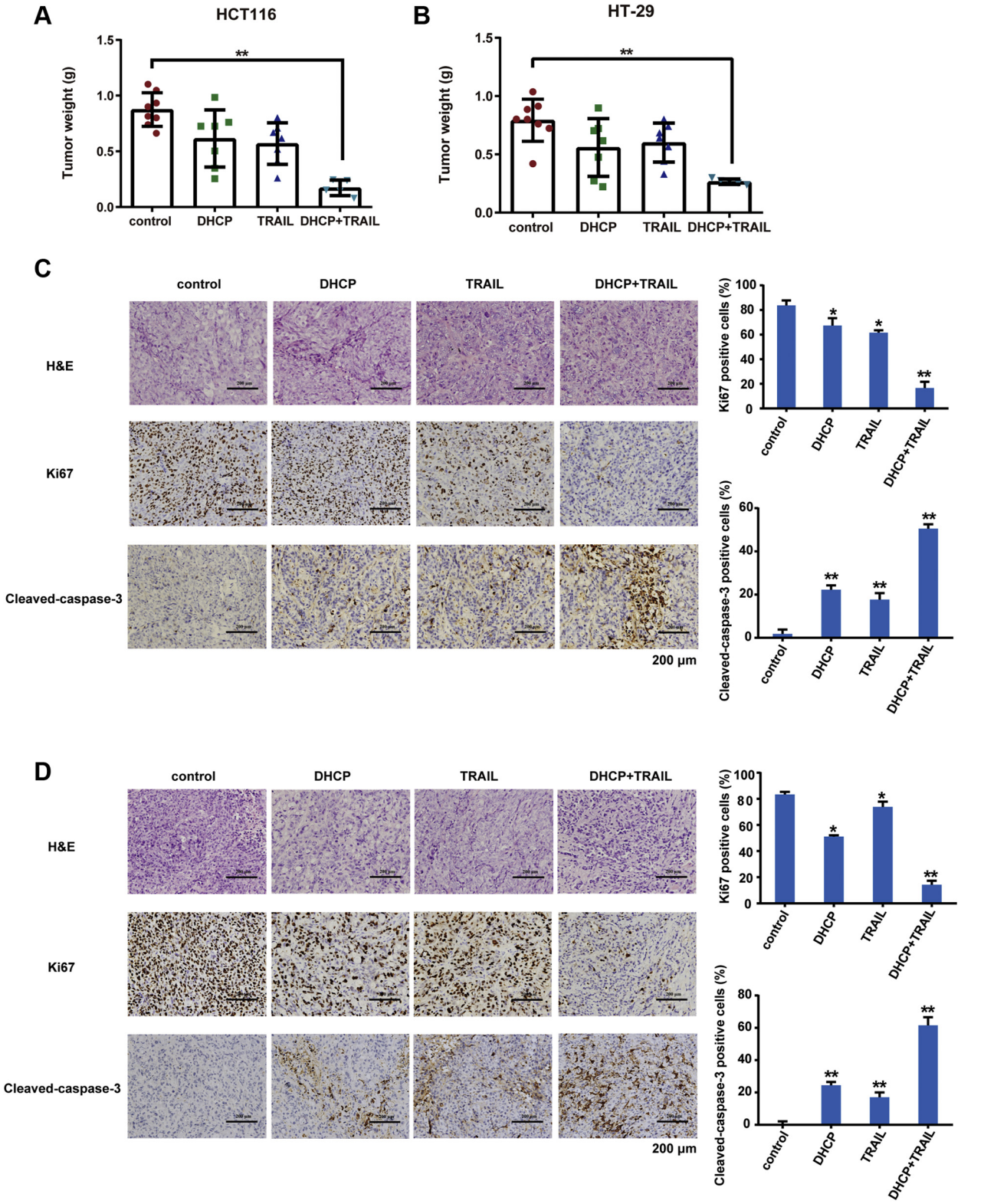

Figure 6. The synergistic effect of DHCP and TRAIL *in vivo*. *A–D*, nude mice bearing HCT116 and HT-29 xenograft tumors were treated with 0.5 mg/kg of DHCP with/without TRAIL (100 μg) every other day. Animals were treated with ten consecutive cycles of the combination therapy regimen. The weights of HCT116 xenograft tumors (*A*) and HT-29 xenograft tumors (*B*) were measured. The expressions of Ki-67 and cleaved-caspase-3 of HCT116 (*C*) and HT-29 (*D*) tumor tissues were tested by immunohistochemistry staining. Statistical significance was determined with Student's *t*-test (*$p < 0.05$, **$p < 0.01$).

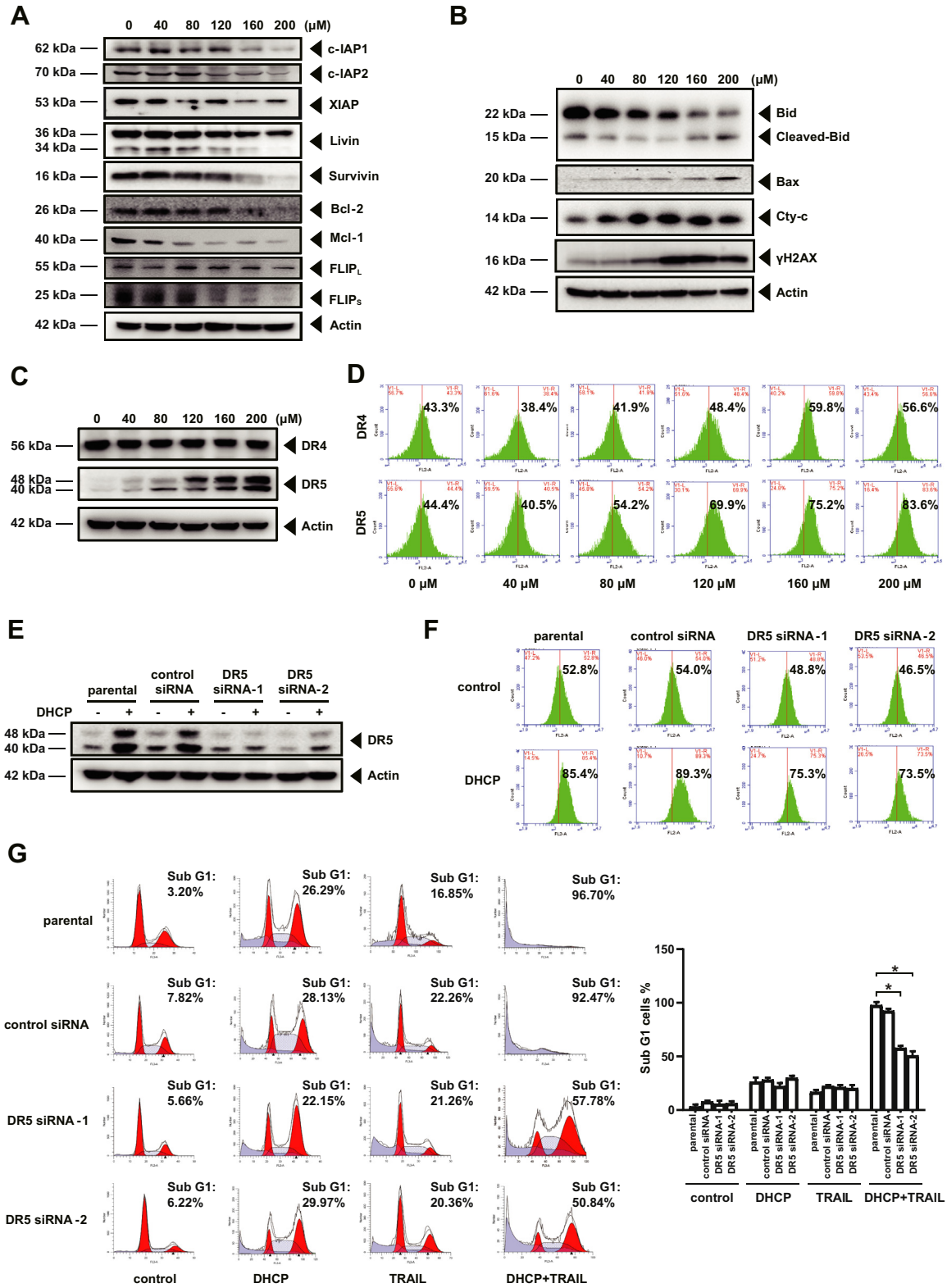

Figure 7. DHCP induces the upregulation of DR5. *A* and *B*, HCT116 cells were treated with indicated concentrations of DHCP for 24 h. The expressions of cell survival proteins (*A*) and procell death proteins (*B*) were detected. *C* and *D*, HCT116 cells were treated with indicated concentrations of DHCP for 24 h. The whole-cell extracts were prepared and subjected to western blot for the analysis of DR4/DR5 proteins (*C*), the surface DR4 and DR5 expression was tested by flow cytometry (*D*). *E* and *F*, HCT116 cells were transfected with control siRNA or DR5 siRNAs, then treated with 200 μM of DHCP for 24 h. The total expression of DR5 (*E*) and the cell surface DR5 expression (*F*) were tested. *G*, HCT116 cells were transfected with control siRNA or DR5 siRNAs, then treated with 200 μM of DHCP with or without 25 ng/ml of TRAIL for 24 h. Cell death was tested by flow cytometry after stained by PI.

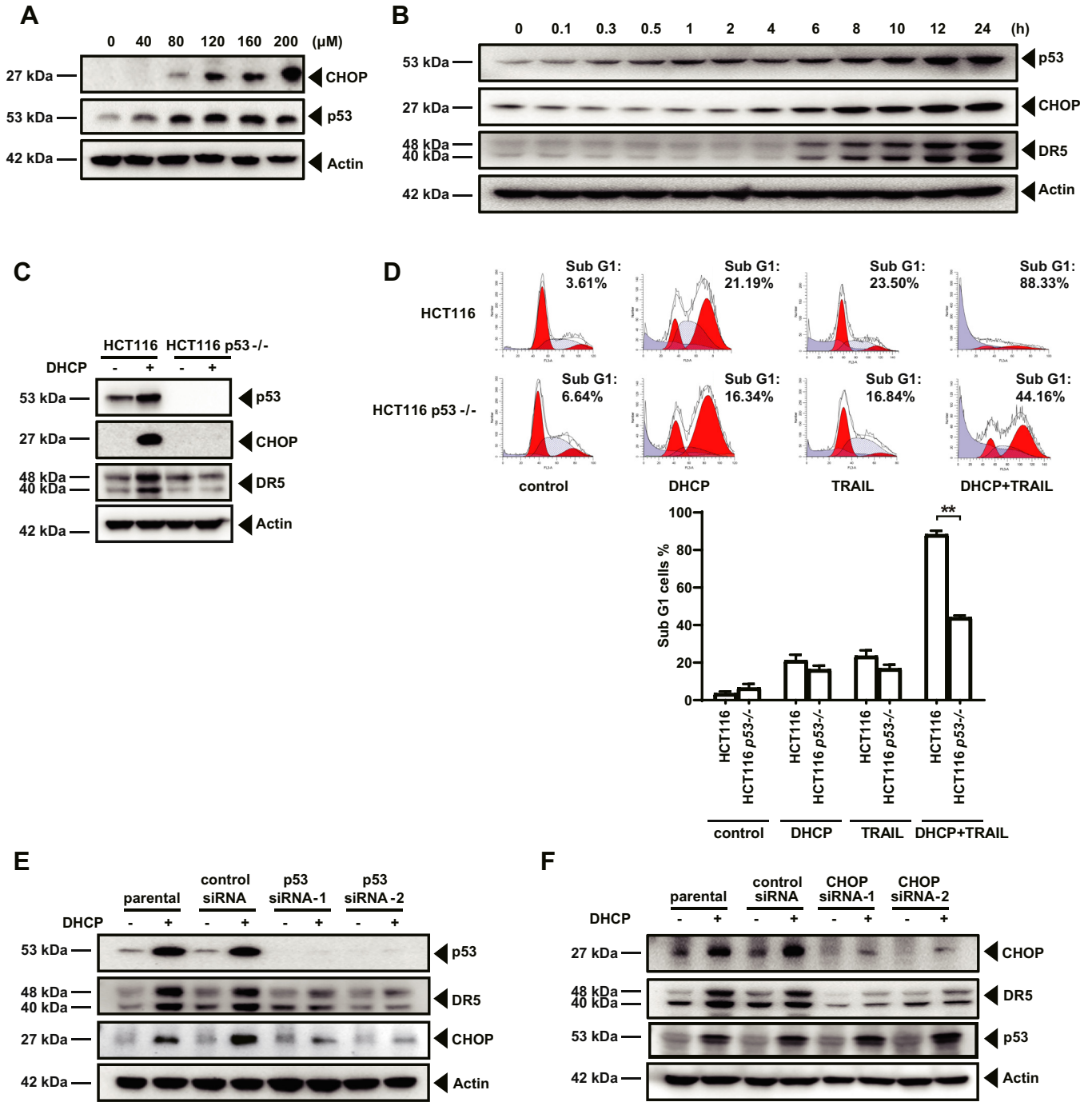

Figure 8. DHCP increases DR5 expression in a p53-CHOP-denpendent pathway. *A* and *B*, HCT116 cells were treated with indicated concentrations of DHCP for 24 h (*A*) or 200 μM of DHCP for indicated times (*B*), then the cells were lysed, and the proteins were tested by western blot. *C*, HCT116 and HCT116 *p53–/–* cells were treated with 200 μM of DHCP for 24 h, whole-cell extracts were prepared and analyzed by western blot. *D*, HCT116 and HCT116 *p53–/–* cells were treated with 200 μM of DHCP with or without 25 ng/ml of TRAIL for 24 h, cell death was analyzed by flow cytometry. *E* and *F*, HCT116 cells were transfected with control siRNA, p53 siRNAs (*E*), or CHOP siRNAs (*F*), then treated with DHCP for 24 h. Whole-cell extracts were prepared and analyzed by western blot.

time-dependent manner (Fig. 8, *A* and *B*), as well as the induction of DR5 in parallel with the increase in p53 and CHOP (Fig. 8*B*). Furthermore, upregulation of DR5 and CHOP induced by DHCP is inhibited in HCT116 *p53–/–* cells (Fig. 8*C*). Moreover, cell death induced by the combination of DHCP and TRAIL was decreased from 88.3% to 44.2% in HCT116 *p53–/–* cells (Fig. 8*D*). To confirm these results, HCT116 cells were transfected with two p53 siRNAs. Consistently, the expression of DR5 was also reduced in p53 siRNAs transfected HCT116 cells (Fig. 8*E*). Furthermore, the expression of CHOP was robustly impacted by p53 siRNAs transfection (Fig. 8*E*).

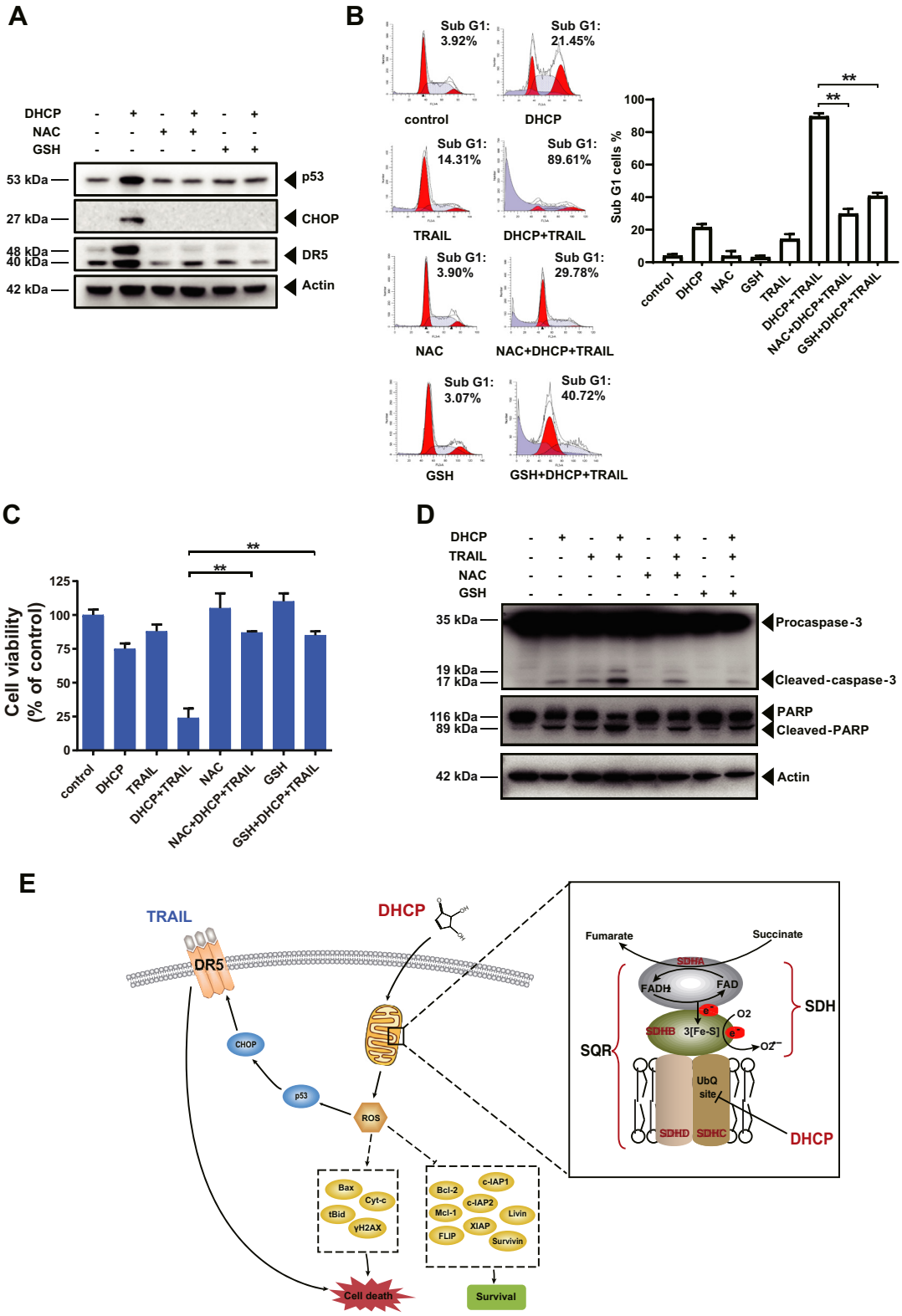

Figure 9. Reactive oxygen species induced by DHCP correlated with the increasing of DR5. *A*, HCT116 cells were pretreated with NAC or GSH for 1 h and then treated with 200 μM of DHCP for 24 h. The expressions of indicated proteins were tested by western blot. *B–D*, HCT116 cells were pretreated with NAC or GSH for 1 h and then cotreated with 200 μM of DHCP and/or 100 ng/ml of TRAIL for 24 h, the cell viability (*B*), cell death (*C*), and proteins expression (*D*) were tested by WST-1 assay, flow cytometry, and western blot, respectively. *E*, an illustration of a likely mechanism of action through which DHCP potentiates TRAIL-induced apoptosis. Statistical significance was determined with Student's *t*-test (*$p < 0.05$, **$p < 0.01$).

ROS induced by DHCP plays a role in p53 and CHOP upregulation

p53, CHOP, and the up-expression of DR5 were also eliminated in the presence of ROS scavengers, NAC or GSH (Fig. 9*A*). Correspondingly, the synergistic effect of DHCP and TRAIL on HCT116 cells was robustly inhibited (Fig. 9, *B–D*). These results indicate that DHCP-induced ROS generation is the root cause of the synergistic effect from the combination of DHCP and TRAIL.

Discussion

The role of dietary components in cancer prevention and progression is an area of increasing clinical and scientific interest. An inverse relation between consumption of fruits and vegetables and the incidence of various cancers has led researchers to investigate the benefits of diet in cancer prevention. Pectin, a family of complex polysaccharides (1), can be found in the peel of citrus fruits, apple pomace, potato, sugar beet pulp, tomato, carrot, etc. (25). Previous reports have shown that pectin can exhibit significant antitumor activities (26). Moreover, the bioavailability and bioactivity of pH- or heat-modified pectin are more effective against cancer (27). However, the requisite bioactive fractions remain unclear. DHCP, isolated from heat-modified citrus pectin (CP), has cytotoxic effects on certain cancer cells (3, 7), but the mechanism accounting for cell death has not been fully elucidated. In this current study, we isolated DHCP from HTCP, and structure elucidation of the effective compound shows its chemical formula to betrans-4,5-dihydroxy-2-cyclopentene-l-one (DHCP).

ROS, which includes superoxide anions (O_2–), hydrogen peroxide (H_2O_2), and hydroxyl radicals (OH·), are intracellular chemical species that are reactive against lipids, proteins, and DNA (20). However, the disproportional increase in intracellular ROS can induce cancer cell cycle arrest, senescence, and apoptosis (22). Production of ROS is elevated in tumor cells, and cell death is triggered when ROS levels are high. In turn, this can be an anticancer strategy to increase cellular ROS levels above the tolerability threshold by utilizing exogenous agents.

The previous research has suggested that ROS-induced cell death can be mediated by the pathway dependence of caspase, ferroptosis, autophagy, pyroptosis, and necroptosis (28). Herein, various types of cell death inhibitors were applied to investigate the pathways involved in DHCP-mediated cell death. The results showed that CRID3, an inhibitor of inflammasomes, could inhibit DHCP-induced cell death. Based on our present knowledge, DHCP increased ROS levels and induced inflammasome-driven pyroptosis (Figs. 2*D* and S9).

In the present study, DHCP was found to lead caspase activation and PARP cleavage. However, the pan caspase inhibitor Z-VAD-FMK could not inhibit DHCP-induced pyroptosis, seems to be a caspase-independent process. Our findings were similar to those results reported by Leclere *et al.* (3, 7). They found that heat-modified citrus pectin (HTCP) induced caspase activation in HepG2 cells, while Z-VAD-FMK also did not inhibit the cell death. Further, they hypothesized that when caspase-3 was inhibited by Z-VAD-FMK, another protease sharing some caspase-3 substrates might be activated and lead to caspase activation and PARP cleavage (3). DHCP is the primary contributor to the activity of HTCP. Hence, we inferred that DHCP might induce a caspase-3-independent pyroptosis, the detailed mechanisms of which are worth to be studied more.

Increased ROS levels are thought to impair the drug resistance of cancer cells (29). Hence, in the present research, we also investigated the sensitizing effect of DHCP with three clinical anticancer drugs (5-fluorouracil, irinotecan, oxaliplatin) and one preclinical drug (TRAIL). Although DHCP can slightly synergize with 5-FU, irinotecan, or oxaliplatin, it does have a highly significant synergistic effect with TRAIL (Fig. S5). TRAIL/Apo2L was discovered as an inducer of apoptosis (30, 31) that, unlike other TNF superfamily members, selectively targets cancer cells while leaving normal cells unharmed (32). Targeting the TRAIL pathway has been of interest in oncology since the 1990s. While the use of TRAIL with increased potency and ability to target cancer cells is a valid approach, it does not address the problem of TRAIL resistance (33). There are numerous TRAIL pathway-resistance mechanisms in cancer, including TRAIL decoys, TRAIL receptor glycosylation, and translocation to the cell membrane. NF-κB, Bcl-XL, Mcl-1, the IAP family, Akt, FLIP, mutation, and loss of caspase-8 expression are also promising combinatorial therapeutics that can address resistance. We are particularly interested in the role of DR5 in this synergistic effect, with the mechanism of action accounting for upregulation of DR5. The reason is that agonistic TRAIL-R antibodies that selectively target DR5 are more attractive for use in humans compared with TRAIL, and several clinical trials investigating TRAIL-R antibodies in solid and hematological tumors have been done.

Furthermore, low-surface expression of TRAIL receptors DR4 and DR5 correlates best with decreased TRAIL sensitivity (34). The combination of TRAIL or TRAIL receptor agonistic targeting with sorafenib is supported mostly in preclinical data. Therapies that induce DNA damage and activate p53, such as chemotherapy and radiation, can upregulate DR4 (35) and have been tested in combination with TRAIL. Strategies to overcome TRAIL resistance associated with low cell surface death receptor levels have also included combinations with histone deacetylase (HDAC) inhibitors (36, 37), proteasome inhibitors (38), and ER stress inducer tunicamycin (39).

In the present study, we found that DHCP enhances TRAIL-induced cell death in HCT116 and HT-29 colon cancer cells and xenograft models, indicating the possibility of DHCP as a promising new TRAIL (or TRAIL-R) antibody sensitizer. On a mechanistic level, DHCP upregulates DR5 expression and procell death proteins and downregulates cell survival proteins that might contribute to DHCP-potentiated TRAIL-induced cell death. Silence of DR5 by siRNA robustly abrogates the synergistic effect of DHCP and TRAIL, indicating the vital role of DR5. We further investigated the mechanism of DHCP

increasing the expression of DR5. Various mechanisms have been reported through which DR5 is upregulated, including ROS generation, p53, CHOP, Sp1, and YY1, activation of ERK1/2, JNK, and NF-κB, etc. (24).In this study, we also identified several mechanisms required for upregulation of DR5 and found that DHCP induces generation of ROS and thereby upregulates p53 and CHOP, ultimately promoting DR5 expression. Here we found that p53 has a role in the expression of DR5. Notably, DHCP can promote TRAIL-induced cell death in colon cancer cells expressing wild-type p53 and mutated p53 (Fig. S6).

Previous studies indicated that intracellular ROS generation contributes to overcoming TRAIL-resistance by DR5 upregulation (40–45). In our present study, DHCP enhanced TRAIL-induced cancer cell apoptosis *via* ROS generation. And p53-CHOP signaling played main role in the upregulation of DR5 triggered by ROS, which was consistent with our previous report (43), in which ginsenoside CK reversed TRAIL resistance by inducing DR5 upregulation *via* ROS provocation and subsequent activation of p53-CHOP pathway. The similar results were found by Kim *et al.* (44) and Yadav *et al.* (45). They found that cellular ROS induced by Zyflamend or cardamonin upregulated DR5 expression through CHOP signal and thereafter sensitized tumor cells to TRAIL-induced apoptosis. Over all the results above, the mechanism of DHCP-sensitized cancer cells to TRAIL-induced cell death might be a general mechanism.

It has been reported that even tumors of the same type from individual patients differ in the number of mutations, which makes tumors unlikely to be treated by agents that target a single gene or a single pathway (46). Fortunately, mitochondria could be a rather invariant target across the various types of neoplastic pathologies. Many agents with anticancer activity that act on mitochondria hold a substantial promise for development into efficient anticancer drugs, because of their selectivity for cancer cells (46). Some of these agents could interfere mitochondrial function to induce ROS generation and induce apoptosis of cancer cells (23, 47). ROS produced by mitochondria is of importance because it could overcome resistance to anticancer drugs (48). The provocation of mitochondrial ROS induced by Z-FL-COCHO or sorafenib sensitizes TRAIL-induced cell death (49, 50). In the present research, DHCP induces the distinct generation of mitochondrial ROS and enhances TRAIL-induced cell death in colon cancer cells (Fig. 9*E*). ROS production is the root cause of DHCP activity. Among mitochondria-target agents, many of them target mitochondrial complexes. Mitochondrial complex II, for example, has been described as a new target for anticancer drugs (46) and has been established as an efficient producer of ROS, along with complexes I and III (51). Enzyme activities of complex II are composed of SDH and SQR activities. Some agents have exhibited antitumor effects by inducing ROS through impairment of SQR activity of mitochondrial complex II without affecting SDH activity. TTFA, an inhibitor of complex II, has been reported to induce apoptosis of U87 and HeLa cells by increasing ROS generation (52). Another study has suggested that TTFA and cisplatin can synergistically stimulate cell death in chemo-resistant neuroblastoma cell lines (53). DHCP exhibits a similar effect with TTFA, suggesting that DHCP such as TTFA is a desirable agent to overcome TRAIL chemo-resistance. Thus, further studies should be carried out to confirm the synergistic effect of TTFA and TRAIL.

Experimental procedures

Reagents and antibodies

CP was purchased from Sigma (P-9135, Sigma Aldrich). Pectinase was purchased from Shandong longke enzyme Co Ltd. His-tagged recombinant human TRAIL (rhTRAIL) was produced and purified as described previously (54). Dulbecco's Modified Eagle Medium (DMEM) (12100-046), Nutrient Mixture F-12 medium (DMEM/F-12) (12400-024), Iscove's Modified Dulbecco's Medium (IMDM) (12200-036) and fetal bovine serum (FBS) (16000-044) were obtained from Gibco. Penicillin/streptomycin (MA0110), Necrostatin-1 (MB5067), Ferrostatin-1 (MB4718), and CRID3 (MB3021) were obtained from meilunbio. U0126 (S1901), SP600125 (S1876), NAC (S0077), GSH (S0073), and Z-VAD-FMK (C1202) were purchased from Beyotime Biotechnology. 3-NPA (N106587) and TTFA (T104976) were obtained from Aladdin. All of the other reagents were of analytical grade or better. The specific antibodies used in this study are described in Table S1.

Preparation of HTCP

HTCP was prepared following published procedures with minor modifications (55). In brief, a 0.5% solution of aqueous pectin dispersion was prepared by dissolving 2 g of CP in 400 ml deionized, filtered water. This solution was autoclaved at 121 °C and 17.2–21.7 psi for 60 min to yield HTCP. At the end of the heat treatment, the solution was allowed to cool to RT and stored overnight at 4 °C, allowing formation of a gel-like precipitate. Then, the aqueous phase and the gel-like precipitate were separated by centrifuging at 12,000 rpm, frozen at −80 °C, and lyophilized, yielding HTCP-P and HTCP-S, respectively.

Fractionation of HTCP

HTCP-S was dissolved in distilled water (10 mg/ml) and dialyzed with a dialysis bag cutoff of 3500 Da, yielding HTCP-S-IS (inside the dialysis bag) and HTCP-S-OS (outside the dialysis bag). HTCP-S-OS was then separated into three components on a Sephadex-G10 column. These three peaks were collected and lyophilized to yield HTCP-S-OS1, HTCP-S-OS2, and HTCP-S-OS3. HTCP-S-OS3 was dissolved in 5% methanol and 0.05% trifluoroacetic acid (TFA) and fractionated on a Shimadzu 10Avp HPLC system equipped with 10Avp HPLC Pump, SPD-10Avp UV-VIS Detector, and RID-10A Refractive Index Detector. The HPLC column was a Kromasil C18 column (4.6 × 250 mm). The material was eluted at a flow rate of 0.6 ml/min using an aqueous solution of 5% methanol (v/v) and 0.05% TFA (v/v), with elution monitored by a refractive index (RI) detector and/or by UV at 235 nm.

The eluate was collected as indicated and lyophilized to yield three fractions denoted as F1, F2, and F3.

HPLC analysis

The lyophilized powder of F3 was dissolved in aqueous solution with 5% methanol (v/v) and 0.05% TFA (v/v) at a concentration of 2.5 mg/ml and analyzed by HPLC using a Kromasil C18 column. The material was eluted using 5% methanol and 0.05% TFA at a rate of 0.6 ml/min, with elution monitored using a RI detector and/or UV detector at 235 nm.

^{1}H NMR spectroscopy

The ^{1}H NMR spectrum of F3 was obtained using a Brűker AV600 spectrometer operating at a ^{1}H frequency of 600 MHz. The F3 sample (10 mg) was dissolved in 0.5 ml MeOD (99.8%), and spectra were acquired at 25 °C using a Bruker 5 mm broadband observe probe. Data were analyzed using standard Brűker software.

MS data

The MS trace of F3 was acquired using an ESI-microTOF instrument covering the m/z range up to 700. Data were analyzed using the Bruker Compass Data Analysis 4.0 software program.

Cell culture

Unless otherwise stated, all cell lines were purchased from American Type Culture Collection and were maintained in the appropriate growth medium at 37 °C and 5% CO_2. HCT116 variants with deletion of *p53* were kindly supplied by Dr Xinshan Ye, (Peking University, Beijing, China). Human lung epithelial A549 cells and A549 ρ0 cells were generously supplied by Dr Qiang Yu (Chinese Academy of Sciences, Shanghai, China). HCT116 and NCM460 cells were cultured in IMDM medium. HT-29 cells were cultured in DMEM/F-12 medium. A549 and HCT116 *p53–/–* cells were cultured in DMEM high-glucose medium. A549 ρ0 cells were cultured in DMEM high-glucose medium with 100 μg/ml pyruvate and 100 μg/ml uridine. All media were supplemented with 10% fetal calf serum, 100 units/ml penicillin, and 100 mg/ml streptomycin.

Cell viability assay

The WST-1 cell proliferation and cytotoxicity assay kit (C0035, Beyotime) was used to measure cell viability. Cells were treated with different concentrations of DHCP, TRAIL, or their combination, for 24 h. The medium was removed and the WST-1 solution was added, and absorbance was measured at 450 nm using a microplate reader (TECAN, infinite F50). All experiments were performed in triplicate and repeated at least three times. Cell viability under each condition is expressed as a percentage of the control set at 100%.

PI staining for DNA fragmentation

Cells were treated with DHCP, TRAIL, or the combination for 24 h. Floating and adherent cells were collected and fixed in 75% ethanol, followed by RNase A (RT405-02, TIANGEN) treatment and propidium iodide (PI) (P4864, Sigma Aldrich) staining. The cells were analyzed on the Accuri C6 flow cytometer (BD Biosciences).

siRNA transfection

Transfection was conducted using the Lipofectamine 3000 transfection reagent (Invitrogen) following the manufacturer's instructions. High-purity controls (scrambled RNA), along with DR5, p53 and CHOP siRNA oligos, were obtained from GenePharma. The targeting sequences of the siRNA constructs are listed in Table S2.

Western blot analysis

Cells were lysed in lysis buffer (50 mM Tris/acetate, pH 7.4, 1 mM EDTA, 0.5% Triton X-100, 150 mM sodium chloride, 0.1 mM PMSF, and Roche incomplete protease inhibitor cocktail). Protein concentrations were measured using the Bradford method. Equal amounts of protein were separated on 12% SDS-PAGE and transferred to PVDF membranes. Then the membrane was blotted with specific antibodies and detected by Tanon-5200 Multi (Tanon, Shanghai, China).

Detection of ROS

Cells were pretreated with or without ROS scavenger for 1 h and then incubated with 200 μM of DHCP for 24 h. The cells were incubated with 10 μM of DCFH-DA (S0033, Beyotime) for 20 min at 37 °C. Fluorescence was measured by using the Accuri C6 flow cytometer (BD Biosciences).

Flow cytometric analysis of the expression of cell surface DR4 and DR5

Cells were treated with different concentrations of DHCP for 24 h, collected, and washed with 2% FBS/PBS. The cells were labeled with anti-DR4 (NB100-56747, Novus Biologicals) or anti-DR5 (NB100-56618, Novus Biologicals) antibody for 20 min on ice and then incubated with phycoerythrin-conjugated secondary antibody for 20 min on ice in the dark. After washing and resuspension in cold 2% FBS/PBS, the cells were analyzed using the Accuri C6 flow cytometer (BD Biosciences).

Measurement of oxygen consumption rate

The mitochondrial OXPHOS function was measured as previously described (21). HCT116 cells were seeded at 50,000/well overnight before running the seahorse experiment. For measuring OCR, cells were pretreated with 200 μM DHCP for 2 h, then incubated with MAS buffer (70 mM sucrose, 220 mM mannitol, 10 mM KH_2PO_4, 5 mM $MgCl_2$, 2 mM Hepes, and 1 mM EGTA; pH 7.2) containing digitonin (0.001%) to permeabilize the plasma membrane selectively. Different oxidizable substrates and inhibitors of ETC complexes were added into different ports of the seahorse cartridge as indicated. O_2 (pmol/min/50,000 cells) consumption rates were measured by Seahorse XFp Extracellular Flux Analyzers (Agilent).

Enzyme assays

The SQR activity and succinate dehydrogenase (SDH) activity were measured as previously described (23). Mitochondria were isolated from HCT116 cells and resuspended in assay buffer (0.3 M mannitol, 25 mM KH_2PO_4, 20 mM succinate, 5 μM rotenone, 2 μM antimycin A, and 10 mM NaN_3, pH 7.4) at 20 μg/ml. The suspension of mitochondria was incubated at room temperature for 10 min, then DHCP, TTFA, or malonate was added and incubated for another 15 min before initiation of reactions, respectively. For SQR activity, reactions were initiated by adding 50 μM decylubiquinone and 50 μM 2,6-dichlorophenolindophenol. The change of absorbance at 600 nm was monitored every minute for 20 min. For the SDH activity, reactions were initiated by adding 150 μM MTT and 400 μM PMS, and the change in absorbance at 570 nm was monitored each minute for 20 min.

Analysis of intracellular ATP levels

Intracellular ATP levels were quantified using an ATP Assay Kit (S0026, Beyotime) according to the manufacturer's instructions. Briefly, cells were incubated with or without DHCP, and harvested, lysed, and centrifuged at 12,000*g* for 10 min at 4 °C. Then 10 μl of supernatant was added to 100 μl of ATP detection buffer, and luminescence was measured using the Spark 10M Multiscan Instrument (TECAN).

Mitochondrial membrane potential

The mitochondrial membrane potential (MMP) was measured using the MMP assay kit with JC-1 (C2006, Beyotime). For this, HCT116 cells were incubated with DHCP at different doses for the indicated times. Then cells were stained with JC-1 at 37 °C for 30 min, and the fluorescence intensity was measured using an Accuri C6 flow cytometer (BD Biosciences).

Mitochondrial complex activity

HCT116 cells were treated with DHCP for 1 h and harvested. The mitochondrial complex activities of HCT116 cells were determined by using the MitoCheck complex activity assay kits (Comin Biotechnology) according to the manufacturer's protocols. Briefly, mitochondria were detached and the mitochondrial pellets were further resuspended in mitochondrial lysis buffer and subjected to ultrasonication to rupture mitochondrial membranes. Protein concentration was measured by the Bradford Protein assay and mitochondrial protein lysate was added to the respective reaction mixture in the 96-well microplate and incubated for indicated times at 37 °C, respectively. The mitochondrial complex activities were normalized by dividing them by protein concentration and expressing as a ration to control. The activity of complex I was determined by the decrease in absorbance at 340 nm corresponding to the oxidation of NADH. The activity of complex II was assessed by coupling the production of ubiquinol to the reduction of the dye DCPIP (2,6-diclorophenol-indophenol), which leads to a decreased absorbance at 605 nm. Complex III (ubiquinol–cytochrome *c* oxidoreductase) activity was quantified by monitored the cytochrome *c* reducing capacity at 550 nm. For the analysis of complex IV, the cytochrome *c* oxidation capability was assessed by measuring the decrease in absorbance at 550 nm. F1F0-ATPase can dephosphorylate ATP to yield ADP and Pi. And F1F0-ATPase activity was determined by measuring Pi increase rate at 600 nm.

Xenograft studies

BALB/c female nude mice (6–8 week old) were injected subcutaneously with 1×10^6 HCT116 or 2×10^6 HT-29 cells mixed with Matrigel (BD Biosciences). Tumors were allowed to develop in the absence of treatment until they were ∼0.2 cm in diameter. For testing the antitumor effect of DHCP alone, mice were treated with DHCP (0.5 mg/kg) by intraperitoneal injection. As a negative control, a subset of mice was injected with saline (vehicle). All animals were treated for three consecutive weeks, and tumor sizes were monitored every week using a caliper to assess tumor volume.

To examine synergistic effects from DHCP and TRAIL, mice were subjected to the DHCP and/or TRAIL treatment regimen. Animals were treated with DHCP (0.5 mg/kg) by intraperitoneal injection with/without purified rhTRAIL (100 μg) by intravenous injection. Animals were treated for three consecutive weeks. Tumor sizes were monitored every week using caliper measurements of tumor volume. All animal experiments were approved by the Animal Care Committee of the Northeast Normal University, China.

Immunohistochemistry

At the end of the xenograft mouse studies, tumors were harvested, fixed, and embedded in paraffin, sectioned and stained with hematoxylin and eosin (H&E), or immunostained with antibodies specific for Ki67 or cleaved-caspase-3. Images were acquired using a fluorescence microscope (Olympus).

Statistical analysis

The SPSS statistical software program was used for all data analyses. Results are expressed as the mean ± SD. Single factor analysis for variance was performed using the ANOVA program, followed by the LSD test. $p < 0.05$ indicates a significant value.

Data availability

All data described are presented either within the article or in the supporting information.

Supporting information—This article contains supporting information.

Acknowledgments—This research was funded by National Science & Technology Major Project "Key New Drug Creation and Manufacturing Program", China (2019ZX09735-001) and the National Natural Science Foundation of China (31770852, 31870796). We are thankful for HCT116 variants with deletion of *p53* gift from

Dr Xinshan Ye, (Peking University, Beijing, China). Dr Qiang Yu (Chinese Academy of Sciences, Shanghai, China) kindly provided human lung epithelial A549 cells and A549 ρ0 cells.

Author contributions—L. C., H. C., and Y. Z. conceived the study. L. C. conducted the majority of the experiments and analyzed the data. M. H. and J. Y. performed the preparation of DHCP. J. Y. and L. S. analyzed the mass spectrometry and ^{1}H NMR spectroscopy data. M. H. provided support in flow cytometry. L. C., H. C., G. T., and Y. Z. wrote the article. H. C. and Y. Z. supervised the project. All the authors discussed the results and commented on the article.

Conflict of interest—The authors declare that they have no conflicts of interest with the contents of this article.

Abbreviations—The abbreviations used are: DCPIP, 2,6-diclorophenol-indophenol; ETC, electron transfer chain; G-3-P, glycerol-3-phosphate; GPDH, glycerol-3-phosphate dehydrogenase; MMP, mitochondrial transmembrane potential; MTT, 3-(4,5-Dimethyl-2-thiazolyl)-2,5-diphenyl-2H-tetrazolium bromide; 3-NPA, 3-nitropropionic acid; OCR, oxygen consumption rate; OXPHOS, oxidative phosphorylation; PMS, phenazine methosulfate; ROS, reactive oxygen species; SDH, succinate dehydrogenase; SQR, succinate ubiquinone reductase; TCA cycle, tricarboxylic acid cycle; TMPD, tetramethyl-p-phenylene diamine; TRAIL, TNF-related apoptosis-inducing ligand; TTFA, 4,4,4-trifluoro-1-(2-thienyl)-1,3-butanedione.

References

1. Leclere, L., Cutsem, P. V., and Michiels, C. (2013) Anti-cancer activities of pH- or heat-modified pectin. *Front. Pharmacol.* **4**, 128
2. Jackson, C. L., Theobald, L. K., Stoffel, M. T., Gao, M. Y., Tran, N. M., Beal, T. L., Dreaden, T. M., Mohnen, D., Kumar, M. V., Eid, M., and Shirley, R. B. (2007) Pectin induces apoptosis in human prostate cancer cells: Correlation of apoptotic function with pectin structure. *Glycobiology* **17**, 805–819
3. Leclere, L., Fransolet, M., Cote, F., Cambier, P., Arnould, T., Van Cutsem, P., and Michiels, C. (2015) Heat-modified citrus pectin induces apoptosis-like cell death and autophagy in HepG2 and A549 cancer cells. *PLoS One* **10**, e0115831
4. Hao, M., Yuan, X., Cheng, H., Xue, H., Zhang, T., Zhou, Y., and Tai, G. (2013) Comparative studies on the anti-tumor activities of high temperature- and pH-modified citrus pectins. *Food Funct.* **4**, 960–971
5. Cheng, H., Li, S., Fan, Y., Gao, X., Hao, M., Wang, J., Zhang, X., Tai, G., and Zhou, Y. (2011) Comparative studies of the antiproliferative effects of ginseng polysaccharides on HT-29 human colon cancer cells. *Med. Oncol.* **28**, 175–181
6. Guan, Y., Zhang, Z., Yu, X., Yan, J., Zhou, Y., Cheng, H., and Tai, G. (2018) Components of heat-treated Helianthus annuus L. pectin inhibit tumor growth and promote immunity in a mouse CT26 tumor model. *J. Funct. Foods* **48**, 190–199
7. Leclere, L., Fransolet, M., Cambier, P., El Bkassiny, S., Tikad, A., Dieu, M., Vincent, S. P., Van Cutsem, P., and Michiels, C. (2016) Identification of a cytotoxic molecule in heat-modified citrus pectin. *Carbohyd. Polym.* **137**, 39–51
8. Wang, S. (2008) The promise of cancer therapeutics targeting the TNF-related apoptosis-inducing ligand and TRAIL receptor pathway. *Oncogene* **27**, 6207–6215
9. Takeda, K., Stagg, J., Yagita, H., Okumura, K., and Smyth, M. J. O. (2007) Targeting death-inducing receptors in cancer therapy. *Oncogene* **26**, 3745–3757
10. Kim, B., Seo, J. H., Lee, K. Y., and Park, B. (2020) Icariin sensitizes human colon cancer cells to TRAIL-induced apoptosis via ERK-mediated upregulation of death receptors. *Int. J. Oncol.* **56**, 821–834
11. Hung, C.-M., Liu, L.-C., Ho, C.-T., Lin, Y.-C., and Way, T.-D. (2017) Pterostilbene enhances TRAIL-induced apoptosis through the induction of death receptors and downregulation of cell survival proteins in TRAIL-resistance triple negative breast cancer cells. *J. Agr. Food Chem.* **65**, 11179–11191
12. Chang, C.-C., Kuan, C.-P., Lin, J.-Y., Lai, J.-S., and Ho, T.-F. (2015) Tanshinone IIA facilitates TRAIL sensitization by up-regulating DR5 through the ROS-JNK-CHOP signaling Axis in human ovarian carcinoma cell lines. *Chem. Res. Toxicol.* **28**, 1574–1583
13. Lee, J.-H., Cho, H.-D., Jeong, I.-Y., Lee, M.-K., and Seo, K.-I. (2014) Sensitization of tumor necrosis factor-related apoptosis-inducing ligand (TRAIL)-Resistant primary prostate cancer cells by isoegomaketone from Perilla frutescens. *J. Nat. Prod.* **77**, 2438–2443
14. Yi, L., Zongyuan, Y., Cheng, G., Lingyun, Z., GuiLian, Y., and Wei, G. (2014) Quercetin enhances apoptotic effect of tumor necrosis factor-related apoptosis-inducing ligand (TRAIL) in ovarian cancer cells through reactive oxygen species (ROS) mediated CCAAT enhancer-binding protein homologous protein (CHOP)-death receptor 5 pathway. *Cancer Sci.* **105**, 520–527
15. Ricci, J. E., Waterhouse, N., and Green, D. R. (2003) Mitochondrial functions during cell death, a complex (I-V) dilemma. *Cell Death Differ* **10**, 488–492
16. Turrens, J. F. (2003) Mitochondrial formation of reactive oxygen species. *J. Physiol-london* **552**, 335–344
17. Bezawork-Geleta, A., Rohlena, J., Dong, L., Pacak, K., and Neuzil, J. (2017) Mitochondrial complex II: At the crossroads. *Trends Biochem. Sci.* **42**, 312–325
18. Sun, X., Ai, M., Wang, Y., Shen, S., Gu, Y., Jin, Y., Zhou, Z., Long, Y., and Yu, Q. (2013) Selective induction of tumor cell apoptosis by a novel P450-mediated reactive oxygen species (ROS) inducer methyl 3-(4-nitrophenyl) propiolate. *J. Biol. Chem.* **288**, 8826–8837
19. Murphy, M. P. (2009) How mitochondria produce reactive oxygen species. *Biochem. J.* **417**, 1–13
20. Quinlan, C. L., Orr, A. L., Perevoshchikova, I. V., Treberg, J. R., Ackrell, B. A., and Brand, M. D. (2012) Mitochondrial complex II can generate reactive oxygen species at high rates in both the forward and reverse reactions. *J. Biol. Chem.* **287**, 27255–27264
21. Zhang, B., Chu, W., Wei, P., Liu, Y., and Wei, T. (2015) Xanthohumol induces generation of reactive oxygen species and triggers apoptosis through inhibition of mitochondrial electron transfer chain complex I. *Free Radic. Bio. Med.* **89**, 486–497
22. Miyadera, H., Shiomi, K., Ui, H., Yamaguchi, Y., Masuma, R., Tomoda, H., Miyoshi, H., Osanai, A., Kita, K., and Ōmura, S. (2003) Atpenins, potent and specific inhibitors of mitochondrial complex II (succinate-ubiquinone oxidoreductase). *P. Natl. Acad. Sci. Usa.* **100**, 473
23. Guo, L., Shestov, A. A., Worth, A. J., Nath, K., Nelson, D. S., Leeper, D. B., Glickson, J. D., and Blair, I. A. (2016) Inhibition of mitochondrial complex II by the anticancer agent Lonidamine. *J. Biol. Chem.* **291**, 42–57
24. Prasad, S., Kim, J. H., Gupta, S. C., and Aggarwal, B. B. (2014) Targeting death receptors for TRAIL by agents designed by Mother Nature. *Trends Pharmacol. Sci.* **35**, 520–536
25. Noreen, A., Nazli, Z. I., Akram, J., Rasul, I., Mansha, A., Yaqoob, N., Iqbal, R., Tabasum, S., Zuber, M., and Zia, K. M. (2017) Pectins functionalized biomaterials; a new viable approach for biomedical applications: A review. *Int. J. Biol. Macromol.* **101**, 254–272
26. Zhang, W., Xu, P., and Zhang, H. (2015) Pectin in cancer therapy: A review. *Trends Food Sci. Tech.* **44**, 258–271
27. Lara-Espinoza, C., Carvajal-Millán, E., Balandrán-Quintana, R., López-Franco, Y., and Rascón-Chu, A. (2018) Pectin and pectin-based composite materials: Beyond food texture. *Molecules* **23**
28. Holze, C., Michaudel, C., Mackowiak, C., Haas, D. A., Benda, C., Hubel, P., Pennemann, F. L., Schnepf, D., Wettmarshausen, J., Braun, M., Leung, D. W., Amarasinghe, G. K., Perocchi, F., Staeheli, P., Ryffel, B., *et al.* (2018) Oxeiptosis, a ROS-induced caspase-independent apoptosis-like cell-death pathway. *Nat. Immunol.* **19**, 130–140

29. Szakács, G., Paterson, J. K., Ludwig, J. A., Booth-Genthe, C., and Gottesman, M. M. (2006) Targeting multidrug resistance in cancer. *Nat. Rev. Drug Discov.* **5**, 219–234
30. Pitti, R. M., Marsters, S. A., Ruppert, S., Donahue, C. J., Moore, A., and Ashkenazi, A. (1996) Induction of apoptosis by Apo-2 ligand, a new member of the tumor necrosis factor cytokine family. *J. Biol. Chem.* **271**, 12687–12690
31. Wiley, S. R., Schooley, K., Smolak, P. J., Din, W. S., Huang, C. P., Nicholl, J. K., Sutherland, G. R., Smith, T. D., Rauch, C., Smith, C. A., *et al.* (1995) Identification and characterization of a new member of the TNF family that induces apoptosis. *Immunity* **3**, 673–682
32. Walczak, H., Miller, R. E., Ariail, K., Gliniak, B., Griffith, T. S., Kubin, M., Chin, W., Jones, J., Woodward, A., Le, T., Smith, C., Smolak, P., Goodwin, R. G., Rauch, C. T., Schuh, J. C., *et al.* (1999) Tumoricidal activity of tumor necrosis factor-related apoptosis-inducing ligand *in vivo*. *Nat. Med.* **5**, 157–163
33. Ralff, M. D., and El-Deiry, W. S. (2018) TRAIL pathway targeting therapeutics. *Expert Rev. Precis. Me.* **3**, 197–204
34. Forero-Torres, A., Varley, K. E., Abramson, V. G., Li, Y., Vaklavas, C., Lin, N. U., Liu, M. C., Rugo, H. S., Nanda, R., Storniolo, A. M., Traina, T. A., Patil, S., Van Poznak, C. H., Nangia, J. R., Irvin, W. J., Jr., *et al.* (2015) Tbcrc 019: A phase II trial of nanoparticle albumin-bound paclitaxel with or without the anti-death receptor 5 monoclonal antibody tigatuzumab in patients with triple-negative breast cancer. *Clin. Cancer Res.* **21**, 2722–2729
35. Guan, B., Yue, P., Clayman, G. L., and Sun, S. Y. (2001) Evidence that the death receptor DR4 is a DNA damage-inducible, p53-regulated gene. *J. Cell. Physiol.* **188**, 98–105
36. Earel, J. K., Jr., VanOosten, R. L., and Griffith, T. S. (2006) Histone deacetylase inhibitors modulate the sensitivity of tumor necrosis factor-related apoptosis-inducing ligand-resistant bladder tumor cells. *Cancer Res.* **66**, 499–507
37. Singh, T. R., Shankar, S., and Srivastava, R. K. (2005) HDAC inhibitors enhance the apoptosis-inducing potential of TRAIL in breast carcinoma. *Oncogene* **24**, 4609–4623
38. Sayers, T. J., and Murphy, W. J. (2006) Combining proteasome inhibition with TNF-related apoptosis-inducing ligand (Apo2L/TRAIL) for cancer therapy. *Cancer Immunol. Immun.* **55**, 76–84
39. Jiang, C. C., Chen, L. H., Gillespie, S., Kiejda, K. A., Mhaidat, N., Wang, Y. F., Thorne, R., Zhang, X. D., and Hersey, P. (2007) Tunicamycin sensitizes human melanoma cells to tumor necrosis factor-related apoptosis-inducing ligand-induced apoptosis by up-regulation of TRAIL-R2 via the unfolded protein response. *Cancer Res.* **67**, 5880–5888
40. Shankar, S., Ganapathy, S., and Srivastava, R. (2008) Sulforaphane enhances the therapeutic potential of TRAIL in prostate cancer orthotopic model through regulation of apoptosis, metastasis, and angiogenesis. *Clin. Cancer Res.* **14**, 6855–6866
41. Shi, Y., Wang, J., Liu, J., Lin, G., Xie, F., Pang, X., Pei, Y., Cheng, Y., Zhang, Y., Lin, Z., Yin, Z., Wang, X., Niu, G., Chen, X., and Liu, G. J. B. (2020) Oxidative stress-driven DR5 upregulation restores TRAIL/Apo2L sensitivity induced by iron oxide nanoparticles in colorectal cancer. *Biomaterials* **233**, 119753
42. Chen, C.-Y., Tai, C.-J., Cheng, J.-T., Zheng, J.-J., Chen, Y.-Z., Liu, T.-Z., Yiin, S.-J., and Chern, C.-L. (2010) 6-Dehydrogingerdione sensitizes human hepatoblastoma Hep G2 cells to TRAIL-induced apoptosis via reactive oxygen species-mediated increase of DR5. *J. Agr. Food Chem.* **58**, 5604–5611
43. Chen, L., Meng, Y., Sun, Q., Zhang, Z., Guo, X., Sheng, X., Tai, G., Cheng, H., and Zhou, Y. (2016) Ginsenoside compound K sensitizes human colon cancer cells to TRAIL-induced apoptosis via autophagy-dependent and -independent DR5 upregulation. *Cell Death Dis.* **7**, e2334
44. Kim, J., Park, B., Gupta, S., Kannappan, R., Sung, B., Aggarwal, B. J. A., and signaling, r. (2012) Zyflamend sensitizes tumor cells to TRAIL-induced apoptosis through up-regulation of death receptors and down-regulation of survival proteins: Role of ROS-dependent CCAAT/enhancer-binding protein-homologous protein pathway. *Antioxid. Redox Sign.* **16**, 413–427
45. Yadav, V. R., Prasad, S., and Aggarwal, B. B. (2012) Cardamonin sensitizes tumour cells to TRAIL through ROS- and CHOP-mediated up-regulation of death receptors and down-regulation of survival proteins. *Br. J. Pharmacol.* **165**, 741–753
46. Neuzil, J., Dong, L. F., Rohlena, J., Truksa, J., and Ralph, S. J. (2013) Classification of mitocans, anti-cancer drugs acting on mitochondria. *Mitochondrion* **13**, 199–208
47. Dong, L. F., Jameson, V. J., Tilly, D., Cerny, J., Mahdavian, E., Marin-Hernandez, A., Hernandez-Esquivel, L., Rodriguez-Enriquez, S., Stursa, J., Witting, P. K., Stantic, B., Rohlena, J., Truksa, J., Kluckova, K., Dyason, J. C., *et al.* (2011) Mitochondrial targeting of vitamin E succinate enhances its pro-apoptotic and anti-cancer activity via mitochondrial complex II. *J. Biol. Chem.* **286**, 3717–3728
48. Wang, H., Gao, Z., Liu, X., Agarwal, P., Zhao, S., Conroy, D. W., Ji, G., Yu, J., Jaroniec, C. P., Liu, Z., Lu, X., Li, X., and He, X. (2018) Targeted production of reactive oxygen species in mitochondria to overcome cancer drug resistance. *Nat. Commun.* **9**, 562
49. Seo, B. R., Min, K. J., Woo, S. M., Choe, M., Choi, K. S., Lee, Y. K., Yoon, G., and Kwon, T. K. (2017) Inhibition of cathepsin S induces mitochondrial ROS that sensitizes TRAIL-mediated apoptosis through p53-mediated downregulation of Bcl-2 and c-FLIP. *Antioxid. Redox Sign* **27**, 215–233
50. Gillissen, B., Richter, A., Richter, A., Preissner, R., Schulze-Osthoff, K., Essmann, F., and Daniel, P. T. (2017) Bax/Bak-independent mitochondrial depolarization and reactive oxygen species induction by sorafenib overcome resistance to apoptosis in renal cell carcinoma. *J. Biol. Chem.* **292**, 6478–6492
51. Ishii, T., Yasuda, K., Akatsuka, A., Hino, O., Hartman, P. S., and Ishii, N. (2005) A mutation in the SDHC gene of complex II increases oxidative stress, resulting in apoptosis and tumorigenesis. *Cancer Res.* **65**, 203–209
52. Chen, Y., McMillan-Ward, E., Kong, J., Israels, S. J., and Gibson, S. B. (2007) Mitochondrial electron-transport-chain inhibitors of complexes I and II induce autophagic cell death mediated by reactive oxygen species. *J. Cell Sci.* **120**, 4155–4166
53. Kruspig, B., Valter, K., Skender, B., Zhivotovsky, B., and Gogvadze, V. (2016) Targeting succinate:ubiquinone reductase potentiates the efficacy of anticancer therapy. *Bba-mol. Cell Res.* **1863**, 2065–2071
54. Kim, S. H., Kim, K., Kwagh, J. G., Dicker, D. T., Herlyn, M., Rustgi, A. K., Chen, Y., and El-Deiry, W. S. (2004) Death induction by recombinant native TRAIL and its prevention by a caspase 9 inhibitor in primary human esophageal epithelial cells. *J. Biol. Chem.* **279**, 40044–40052
55. Koyama, N., Sagawa, H., Kobayashi, E., Enoki, T., Hua-kang, WU, Nishiyama, E., Ikai, K., and Kato, I. (2000) Cyclopentenones, process for preparing the same, and the use thereof. US patent, US6087401